Title

Collagen crosslinking impacts stromal wound healing and haze formation in a rabbit phototherapeutic keratectomy model.

Authors

Moore, Bret

Jalilian, Iman

Kim, Soohyun

et al.

Publication Date

2023

Peer reviewed

Molecular Vision 2023; 29:102-116 <http://www.molvis.org/molvis/v29/102>
Received 16 August 2022 | Accepted 14 July 2023 | Published 16 July 2023

Collagen crosslinking impacts stromal wound healing and haze formation in a rabbit phototherapeutic keratectomy model

Bret A. Moore,[1] Iman Jalilian,[2] Soohyun Kim,[2] Makiko Mizutani,[2] Madison Mukai,[2] Connor Chang,[2] Alec M. Entringer,[3] Kamesh Dhamodaran,[4] Vijay Krishna Raghunathan,[3,4] Leandro B. C. Teixeira,[5] Christopher J. Murphy,[2,6] Sara M. Thomasy[2,6]

[1]Department of Small Animal Clinical Sciences, College of Veterinary Medicine, University of Florida, Gainesville, FL; [2]Department of Surgical and Radiological Sciences, School of Veterinary Medicine, University of California-Davis, Davis, CA ; [3]Department of Biomedical Engineering, Cullen College of Engineering, University of Houston, Houston, TX; [4]Department of Basic Sciences, College of Optometry, University of Houston, Houston, TX ; [5]Department of Pathobiological Sciences, School of Veterinary Medicine, University of Wisconsin-Madison, Madison, WI ; [6]Department of Ophthalmology & Vision Science, School of Medicine, University of California-Davis, Sacramento, CA

Purpose: The purpose of this study was to evaluate the elastic modulus, keratocyte-fibroblast-myocyte transformation, and haze formation of the corneal stroma following combined phototherapeutic keratectomy (PTK) and epithelium-off UV-A/riboflavin corneal collagen crosslinking (CXL) using an in vivo rabbit model.
Methods: Rabbits underwent PTK and CXL, PTK only, or CXL 35 days before PTK. Rebound tonometry, Fourier-domain optical coherence tomography, and ultrasound pachymetry were performed on days 7, 14, 21, 42, 70, and 90 post-operatively. Atomic force microscopy, histologic inflammation, and immunohistochemistry for α-smooth muscle actin (α-SMA) were assessed post-mortem.
Results: Stromal haze formation following simultaneous PTK and CXL was significantly greater than in corneas that received PTK only and persisted for more than 90 days. No significant difference in stromal haze was noted between groups receiving simultaneous CXL and PTK and those receiving CXL before PTK. Stromal inflammation did not differ between groups at any time point, although the intensity of α-SMA over the number of nuclei was significantly greater at day 21 between groups receiving simultaneous CXL and PTK and those receiving CXL before PTK. The elastic modulus was significantly greater in corneas receiving simultaneous CXL and PTK compared with those receiving PTK alone.
Conclusions: We showed that stromal haze formation and stromal stiffness is significantly increased following CXL, regardless of whether it is performed at or before the time of PTK. Further knowledge of the biophysical cues involved in determining corneal wound healing duration and outcomes will be important for understanding scarring following CXL and for the development of improved therapeutic options.

Corneal collagen crosslinking (CXL) is a minimally invasive procedure that consists of a photochemical reaction between riboflavin and the corneal stromal collagen fibers using the energy of ultraviolet light (UV-A) [1-3]. The primary goal of CXL is to increase the mechanical strength of the corneal stroma through the formation of additional crosslinks between collagen fibers and/or proteoglycan core proteins and was initially used as a means to treat keratoconus [1,4-7]. Since first being described 20 years ago, CXL remains the only known treatment to stop the progression of corneal ectasia [8,9]. The use of CXL in combination with keratorefractive procedures to increase the mechanical strength of the cornea is quickly growing as a means to reduce the incidence of the development of corneal ectatic diseases post-operatively [1-3,7] as well as to prevent myopic or hyperopic regression post refractive surgery [9,10].

Generally, CXL performed in conjunction with keratorefractive surgery has been reported to have infrequent post-operative complications, most of which were related to planned procedural epithelial debridement and included pain [11], keratitis [12-16], persistent epithelial defects [17], and keratomalacia [9,18-20]. Corneal opacity has frequently been described post-CXL and keratorefractive surgery, mostly due to early corneal edema and stromal haze [21,22]. It is well documented that biophysical cues such as stiffness and topography influence corneal stromal cell behavior, and that increased stiffness may promote the transformation of resident stromal keratocytes to fibroblasts and subsequently myofibroblasts (keratocyte–fibroblast–myocyte, KFM, transformation) [23-26]. Additionally, it has been shown that the corneal wound changes in stiffness over time and that it precedes the occurrence of myofibroblasts during wound repair [26]. However, the biophysical effects of CXL and the

Correspondence to: Sara M. Thomasy, UC Davis School of Veterinary Medicine, Department of Surgical and Radiological Sciences, 1220 Tupper Hall, University of California, Davis, Davis, CA 95616; email: smthomasy@ucdavis.edu

Table 1. Summary of experimental groups and timeline of procedures.

Groups	Day −35	Day 0	Day 21	Day 90
Group 1A (n=8)	-	Epithelial debridement + PTK + CXL	Euthanize (n=4)	Euthanize (n=4)
Group 1B (n=8)	-	Epithelial debridement + PTK	Euthanize (n=4)	Euthanize (n=4)
Group 2A (n=8)	Epithelial debridement + CXL	PTK	Euthanize (n=4)	Euthanize (n=4)
Group 2B (n=8)	Epithelial debridement	PTK	Euthanize (n=4)	Euthanize (n=4)

biophysical cues responsible for the development of corneal haze by alteration of the stromal microenvironment during corneal wound healing following CXL have not been fully understood or identified.

The aims of the present study are to evaluate the elastic modulus of the corneal stroma, KFM transformation, and stromal haze formation following keratorefractive surgery (phototherapeutic keratectomy, PTK) combined with CXL using a rabbit model. By so doing, the goal is to determine whether stiffening the corneal stromal matrix by CXL before laser ablation via PTK has a similar or different effect to performing CXL immediately after PTK. First, it is hypothesized that concurrent CXL and PTK increase local corneal stiffness, and thus stromal haze formation. Second, it is hypothesized that CXL performed before PTK increases local corneal stiffness and results in increased stromal haze formation relative to PTK without CXL by promoting myofibroblast formation in the wound space.

METHODS

Animals and study design: All aspects of the study and design were approved by the Institutional Animal Care and Use Committee (IACUC #19763) of the University of California, Davis, and performed according to the Association for Research in Vision and Ophthalmology resolution on the use of animals in research. Thirty-two female New Zealand White rabbits (Charles River Laboratories, Wilmington, MA) 4 months of age were used. Prior to inclusion in the study, all rabbits had undergone complete ophthalmic examination, including slit lamp biomicroscopy (Kowa SL-15, Kowa, Tokyo, Japan) and indirect ophthalmoscopy using a 2.2D panretinal indirect lens (Volk Optical Inc., Mentor, OH, USA) and a portable headset (Keeler AllPupil II LED Vantage Plus Wireless Headset, Keeler Instruments Inc., Broomall, PA, USA), rebound tonometry (Tonolab, Icare Finland Oy, Vantaa, Finland), Fourier-domain optical coherence tomography (FD-OCT; RTVue 100, software version 6.1, Optovue Inc., Fremont, CA, USA), ultrasonic pachymetry (USP; Accupach VI, Accutome Ultrasound Inc., Malvern, PA, USA), and fluorescein staining of the cornea, as described previously [26]. All animals were free of ophthalmic disease at the initiation of the study.

The rabbits were randomly assigned to one of four groups, with a total of eight rabbits per group. Evaluators (BAM, SK) were masked to the group and individual identity of each rabbit. Group 1A rabbits underwent PTK OD immediately followed by CXL OD at day 0. Group 1B rabbits served as the control population and had only PTK OD at day 0. Group 2A rabbits underwent CXL OD at day −35 and then underwent PTK at day 0. Group 2B rabbits served as a second control population, receiving only an epithelial debridement at day −35 then PTK performed at day 0. The left eye served as an untreated control in each animal of all groups. The study design is shown in Table 1.

Following all surgical procedures, slit lamp biomicroscopy and indirect ophthalmoscopy using the 2.2D panretinal indirect lens and portable headset, rebound tonometry, FD-OCT (26,000 A scan/sec, 5 µm axial resolution, 840 nm superluminescent diode), USP, and fluorescein staining of the cornea was performed. FD-OCT of the central cornea was performed using a corneal adaptor module. Thickness of the cornea and amount of haze were measured using the RTVue measuring tool.

Additionally, all rabbits were monitored for pain twice daily, evidenced by blepharospasm. If a rabbit was deemed painful, pain control was initiated with buprenorphine (Reckitt Benckiser Healthcare, Hull, England, UK) q12h by mouth followed by re-assessment the following day before administration. Rabbits were also maintained on a topical broad-spectrum antibiotic that is without systemic concerns for administration in rabbits (ofloxacin 0.3% solution, Akorn Inc., Lake Forest, IL) twice daily post-operatively until the affected cornea was confirmed to have healed by a negative fluorescein stain.

Epithelial debridement and excimer laser PTK: All the surgical and post-operative procedures briefly described below were performed as previously detailed [26]. Briefly, pre-anesthetic medication consisted of intramuscular midazolam (0.7 mg/kg) and hydromorphone (0.1 mg/kg). Induction proceeded and was maintained with the

intramuscular administration of 10–30 mg/kg of ketamine. Proparacaine hydrochloride 0.5% ophthalmic solution (Bausch and Lomb, Rochester, NY, USA) was administered topically. Epithelial debridement was demarcated using an 8 mm trephine in the central cornea OD and removed using an excimer spatula (BD Vistitec, Franklin Lates, NJ, USA). A PTK (6 mm diameter, 40 Hz, 167 pulses, 100 µm depth) was performed using an excimer laser (Nidek Excimer Laser Corneal Surgery System EC-5000, Fremont, CA) in the center of the epithelial wound. The rationale for the use of PTK over other keratoretractive surgical modalities (e.g., LASIK) was because PTK is an excellent model for evaluating the severity and distribution of stromal haze and stiffness, and the PTK model had been optimized by the author's laboratory in previous studies [26]. Following post-operative examinations and scoring for the first week after surgery, a slit lamp examination was performed with the semiquantitative preclinical ocular toxicology scoring (SPOTS) system [27] with an additional scoring component for stromal haze [28]. In addition, the aforementioned examinations and scoring with rebound tonometry, FD-OCT, USP, and fluorescein staining were performed on days 7, 14, 21, 42, 70, and 90 following PTK in the Group 1 rabbits. The Group 2 rabbits received the same post-operative treatments as the Group 1 rabbits following both day −35 and day 0 surgeries. Between day −35 and day 0, no imaging or examinations beyond the week of postoperative SPOTS scoring took place. Examinations and imaging were then performed immediately before and following surgery on day 0 and again followed by the scoring and imaging schedule detailed for Group 1.

Corneal collagen crosslinking: CXL was performed under general anesthesia. Eyelids were retracted using a Barraquer wire speculum. One drop of aqueous 0.1% riboflavin sodium phosphate (Jiang'Xi Pharmaceutical Co. Ltd., China) was instilled topically on the cornea (epithelium removed) at 2-min intervals for 30 min before introduction of UV-A light. A UV-A light source (OmniCure S1000, Lumen Dynamics, Mississauga, Ontario, Canada) of 365 nm at an irradiance of 3 mW/cm^2 (total dose of 5.4 J/cm^2) was focused over the cornea for 30 min, with riboflavin administration every 2 min. Following the procedure, a single drop of 0.5% proparacaine (Alcon Inc., Fort Worth, TX, USA) was applied topically to the cornea.

Tissue harvest and processing: Chosen at random, one half of each group was euthanized on day 21 and the other half on day 90, immediately following examination and imaging. The rabbits were euthanized with pentobarbital (200 mg/kg, IV), as previously described by our group [26]. From them, 8 mm central corneal buttons were harvested and divided into four equal 2 mm sections; of these, two sections were immediately processed for atomic force microscopy (AFM), one section was placed in 10% neutral buffered formalin for histologic sectioning and light microscopy and immunohistochemistry, and one section was placed in Karnovsky's glutaraldehyde solution for potential future transmission electron microscopy (TEM), which was elected not to be pursued at this time due to availability. The corneal stroma was exposed for AFM with an epithelial debridement and 15-micron PTK, as previously described [26].

Atomic force microscopy: Atomic force microscopy (AFM) was performed to measure the elastic modulus of the corneal stroma, as previously detained by our group [26,29]. Briefly, force versus indentation curves were obtained using the MFP-3D Bio AFM (Asylum Research, Santa Barbara, CA) mounted on a Zeiss Axio Observer inverted microscope (Carl Zeiss, Thornwood, NY). To functionalize the cantilever, a dry borosilicate glass bead with a nominal radius of 4.6–5.9 µm (Thermo Scientific, Fremont, CA) was glued to the end of a silicon nitride PNP-TR-50 cantilever with an actual spring constant (κ) of 55–246 pN nm^{-1} and length of 100 µm (Nano World, Switzerland). The deflection sensitivity of the probes was measured by taking the average of five force curves on a glass slide in DPBS. The spring constant of each cantilever probe used for the indentation measurements was determined using a thermal tuning method. To measure the stiffness of the rabbit corneas, corneal sections were adhered to the AFM dishes using cyanoacrylate glue. All samples were equilibrated in HBSS for at least 60 min before obtaining measurements to minimize thermal drift. For all samples, five force curves at 2 µm s^{-1} were obtained from five to 10 random positions. The elastic modulus (E) of each sample was obtained by fitting the indentation force versus the indentation depth of the sample and further by applying the Hertz model for a spherical tip, as shown in Equation (1),

$$F = \frac{4}{3}\frac{E}{(1-\nu^2)}\delta^{3/2}\sqrt{R}$$

where F is the force applied by the indenter, E is Young's modulus, ν is Poisson's ratio (assumed to be 0.5 for biologic samples) [30], δ is the indentation depth, and R is the radius of curvature of the sphere.

Histopathology and immunohistochemistry: Formalin-fixed samples were embedded in paraffin and sectioned, with 10 um sections mounted on each slide. One slide of each rabbit cornea from days 21 and 90 was stained with hematoxylin and eosin (H&E, Fisher Scientific, Carlsbad, CA) before light microscopy. Slides were reviewed and scored by a board-certified veterinary pathologist (LBCT), who was masked to

group assignments, for inflammation (scores between 0 to 3) based on severity, predominant inflammatory cell type, and location. The following inflammatory scores were given: 0 when rare or absent inflammatory cells were noted; 1 when low numbers of scattered inflammatory cell aggregates were observed; 2 when focally large or diffusely moderate numbers of inflammatory cells were present (+/− distortion of tissue architecture); and 3 when large populations of inflammatory cells caused effacement and/or distortion of the mucosa/epithelium.

Another slide from each sample was processed for immunohistochemistry. Paraffin-embedded samples were sectioned at 5 µm thickness using a microtome and mounted on Superfrost microscope slides (Fisher Scientific). For immunostaining, paraffin sections were heated in citrate buffer (10 mM sodium citrate, 0.05% Tween-20, pH 6) for 30 min using a steamer for antigen retrieval. Paraffin sections were blocked and incubated with mouse anti-α-smooth muscle actin antibody (1:800; Sigma-Aldrich) at 4 °C overnight. Sections were then stained with AlexaFluor 594-conjugated goat anti-mouse secondary antibody (1:500, Invitrogen). The samples were counterstained with DAPI and mounted with ProLong Gold Antifade mountant (Invitrogen). Slides were imaged using a Leica DMi8 fluorescence microscope (Leica Microsystems, IL). The full diameter of each cornea was imaged using a 20× APO-PLAN objective with identical exposure settings and stitched together to visualize the entire section. Two sections per animal per time point were stained with the desired antigen, and one section served as a negative control. The number of nuclei was counted by the particle analysis algorithm on the DAPI channel using LASX software (Leica Microsystems). Background fluorescence intensity was determined from negative control samples in the 594 nm channel and used to subtract from all tissue samples. Fluorescence intensity of the α-SMA signal (594 nm channel) within the anterior stroma (150 µm stromal depth) was quantified using LASX software. The percentage of α-SMA positive cells was then calculated as a function of the total area for each sample.

Statistical analysis: Data were presented as mean ± standard deviation (SD), and statistical analysis was performed with GraphPad Prism 7.03 (GraphPad Software Inc., San Diego, CA). The histopathology data were analyzed by the Kruskal–Wallis test followed by Dunn's multiple comparisons test. Other data sets were compared by repeated measure two-way ANOVA. When variability between the data set means was determined to be significant, Tukey's or Sidak's multiple comparisons test was used to compare these data sets. Values of $p < 0.05$ were considered statistically significant.

RESULTS

Central corneal thickness: Central corneal thickness (total - CCT) measured with the FD-OCT images significantly increased after CXL in both Groups 1 and 2 (Figure 1). The CCT of Group 1A at day 7 (398 ± 82 µm; $p < 0.001$) and day 21 ($p < 0.001$) was significantly thicker than Group 1B at the same time points. The CCT in Group 1B was significantly thinner than baseline from day 0 ($p = 0.03$) following PTK to day 21 (377 ± 51 µm; $p < 0.001$). However, there were no significant differences in CCT between time points compared with the baseline in Group 1A. In Group 2, the CCT of Group 2A was significantly thicker than that of Group 2B after the CXL (day −35; 520 ± 40 µm, $p < 0.001$), but no significant differences were found between Groups 2A and 2B at any other time point. CCT after PTK was significantly thinner than the baseline thickness at days 0 and 7 in both Group 2A (281 ± 43 µm at day 0 and 277 ± 44 µm at day 7; $p < 0.001$ at both day 0 and day 7) and Group 2B (291 ± 54 µm at day 0, $p = 0.02$, and 289 ± 41 µm at day 7, $p = 0.01$).

Corneal epithelium: In Group 1, the mean time to corneal epithelial wound closure was 5.9 ± 2.0 and 5.5 ± 1.2 days in Group 1A and Group 1B, respectively ($p = 0.661$). In Group 2 (CXL performed before PTK), corneal epithelial wound healing was completed at 3.0 ± 0.0 and 3.4 ± 0.5 days after epithelial debridement following CXL (Group 2A) or no treatment (Group 2B), respectively, with no significant differences ($p = 0.080$). The time to healing of the corneal epithelial wound after PTK was similar to Group 1, at 5.3 ± 1.0 and 6.0 ± 0.0 days in the CXL (Group 2A) and control (Group 2B), respectively ($p = 0.251$). Two eyes of Group 1A showed small re-ulcerations of the central cornea, which healed uneventfully. The epithelial wound area versus time curve showed no significant differences between groups ($p = 0.33$; Figure 2).

Corneal stroma: Clinical assessment of stromal haze: Transient conjunctival hyperemia, chemosis, and iris hyperemia were observed in all groups at days 1–3 post CXL and/or PTK. Clinical assessment of the density of stromal haze by slit lamp biomicroscopy (stromal haze SLB) was significantly increased from day 7 post PTK ($p < 0.001$) and remained significantly higher than baseline until day 90 ($p < 0.001$) in all groups (Figures 3 and 4). Peak density of stromal haze was day 42 across all groups. Stromal haze SLB of eyes in group 1A was significantly denser than in Group 1B at days 21, 42, 70, and 90 ($p < 0.01$). However, no significant differences in the stromal haze scores were observed between Groups 2A and 2B from day 7 until day 90 ($p = 0.300$). Additionally, stromal haze SLB was significantly greater in Group 1A versus Group 2A from day 21 post PTK ($p = 0.003$).

The amount of stromal haze (Figure 5), assessed by the percentage of the stromal thickness affected, as measured by FD-OCT (stromal haze OCT), differed significantly between Groups 1A and 1B at day 7 (p <0.001), day 21 (p <0.001), day 42 (p <0.001), and day 70 (p <0.001). In Group 2, the percentage of stromal haze OCT thickness of the CXL eyes (Group 2A) was significantly higher than in the control eyes (Group 2B) until day 42; that is, 82.9 ± 12.8 in Group 2A and 9.5 ± 17.6 in Group 2B (p <0.001) at day 0 before PTK, 75.8 ± 23.4 in Group 2A and 27.1 ± 18.3 in Group 2B at day 7 (p <0.001), 74.8 ± 20.4 in Group 2A and 22.1 ± 4.8 in Group 2B at day 21 (p <0.001), and 67.8 ± 22.4 in Group 2A and 26.8 ±

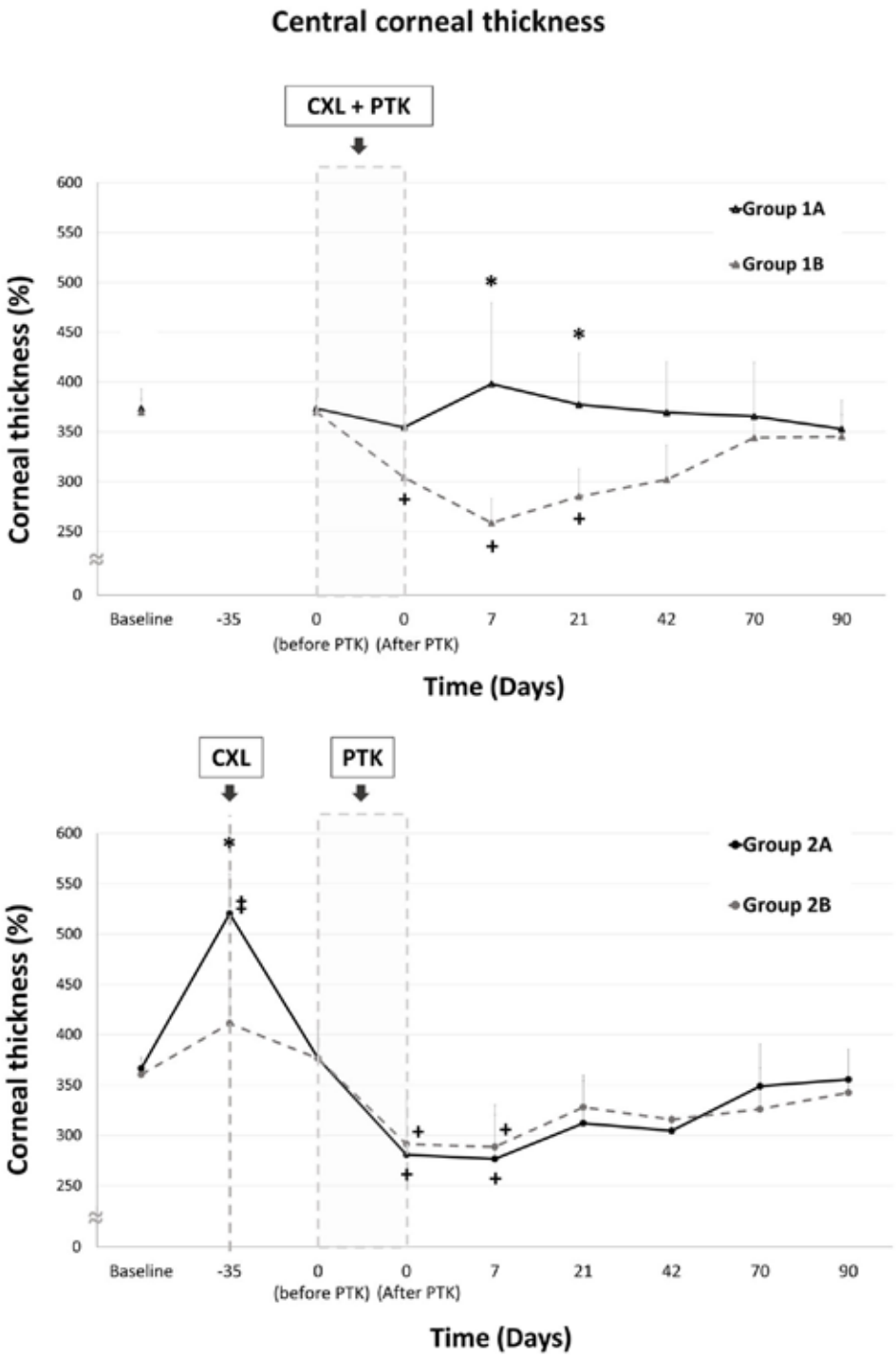

Figure 1. Central corneal thickness (total - CCT) as a function of time. CCT was transiently increased after CXL in both groups. The CCT after CXL was significantly (*) thicker than in controls in both Groups 1 and 2 at the indicated time points. The CCT was significantly increased from the baseline in Group 2A after the CXL (‡) and significantly decreased from the baseline in Groups 1B, 2A, and 2B after the PTK (+). P <0.05, all statistics conducted with the repeated measure two-way ANOVA followed by Sidak's multiple comparisons test.

1.7 in Group 2B at day 42 (p = 0.032). However, there were no significant differences between Group 1A and Group 2A at any time point (p = 0.385).

Corneal stroma: Histologic assessment of inflammation: Inflammation was present in 75% of Group 1A corneas, compared with only 25% of corneas in all other groups, 21 days post PTK. However, there were no significant differences between groups (p = 0.11). Inflammatory cells were predominantly polymorphonuclear cells in all cases, except for one cornea in Group 1A, in which predominantly mononuclear cells were noted. Inflammation had completely

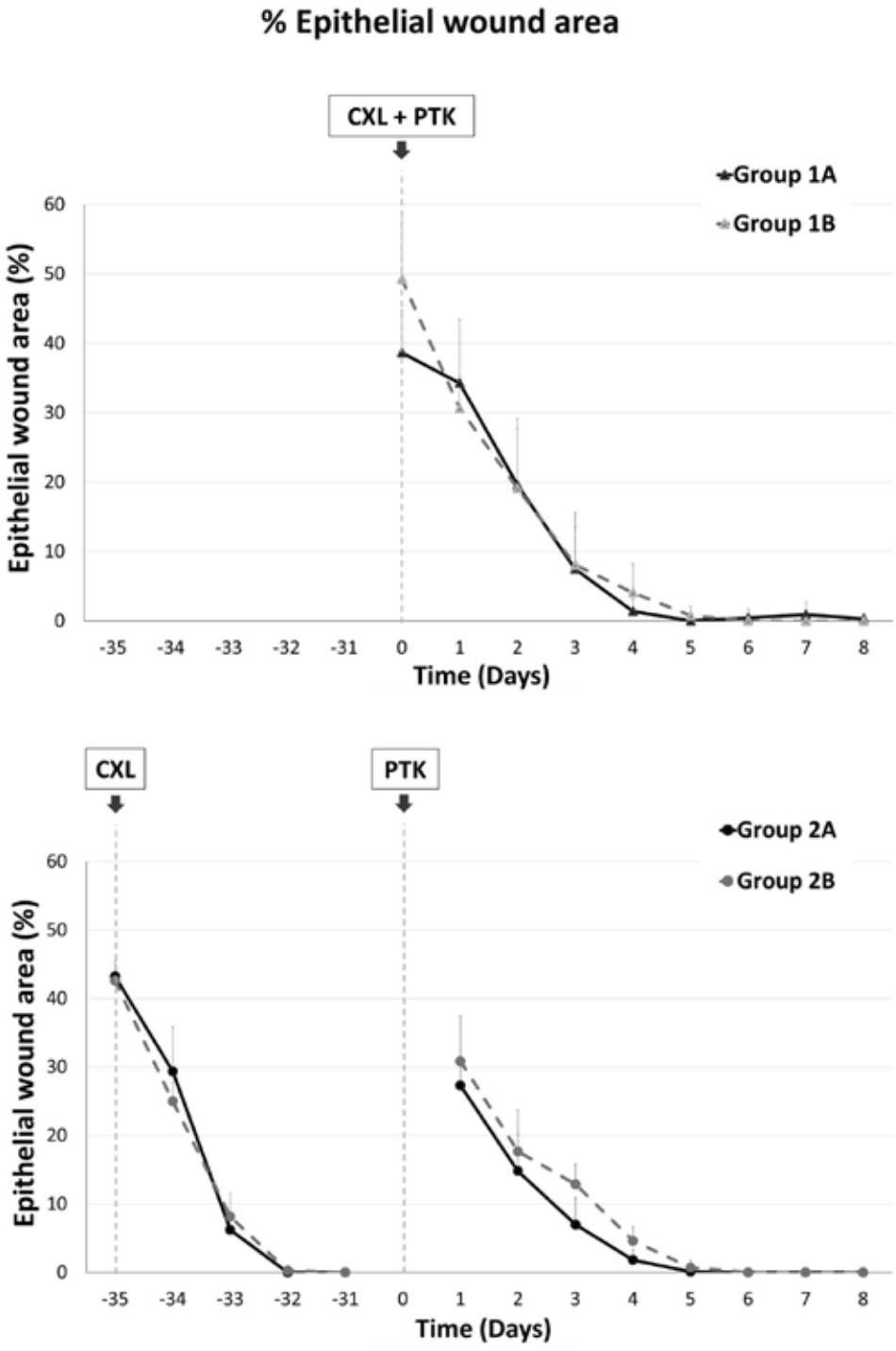

Figure 2. Percentage epithelial wound area showed no significant differences between groups. P = 0.33, repeated measure two-way ANOVA followed by Tukey's multiple comparisons test.

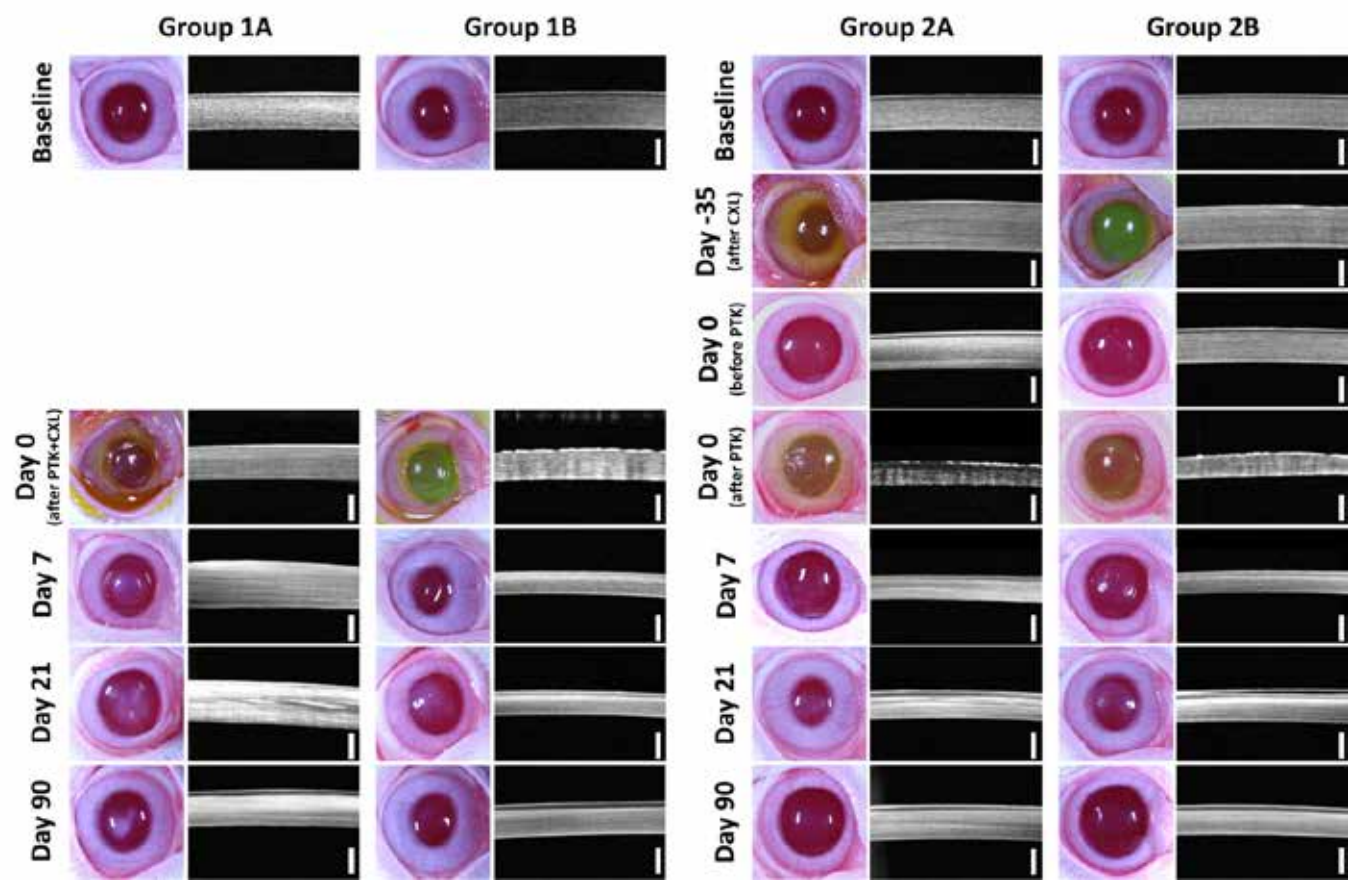

Figure 3. Representative color photographs and OCT images of a single rabbit in each group at baseline and days −35, 0, 7, 21, and 90. Marked stromal haze was observed until day 90 in Group 1A. Scale bar represents 250 µm.

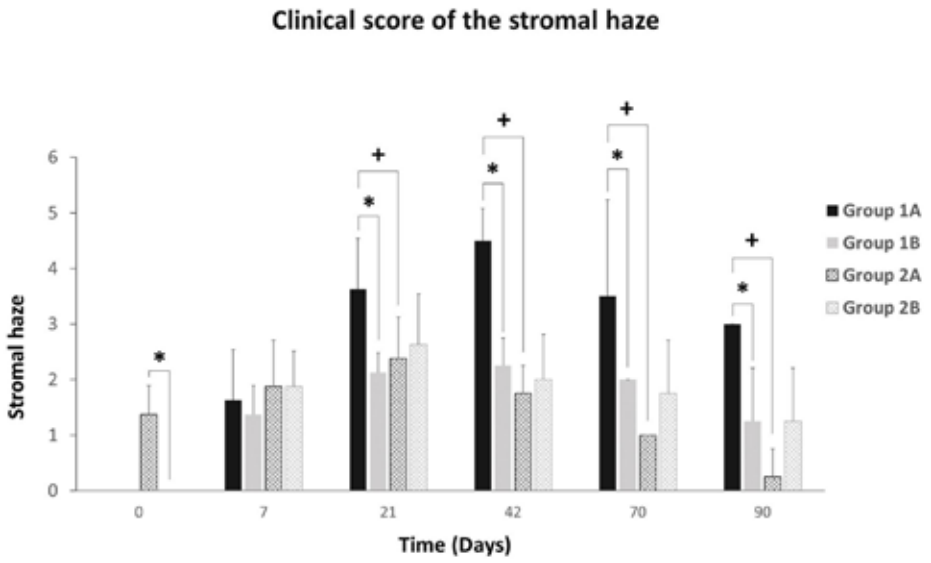

Figure 4. Clinical score of the stromal haze. Stromal haze was significantly higher in Group 1A at days 21–90 post PTK than in Groups 1B (*) and 2A (+). *, + p <0.05, repeated measure two-way ANOVA followed by Tukey's multiple comparisons test.

regressed by day 90 in all corneas. Neovascularization was not noted in any cases.

Corneal stroma: Immunohistochemistry: The intensity of the α-SMA (intensity/mm^2) immunofluorescence over the number of nuclei was significantly higher in Group 1A corneas than in Group 2A ($p = 0.01$) and 2B ($p = 0.01$) corneas at day 21; however, no significant differences were detected among all groups by day 90 (Figure 6).

Corneal stroma: Elastic modulus of corneal stroma: The elastic modulus of the rabbit corneas that received CXL and PTK on a same day (Group 1A) was significantly greater (4.54 ± 0.65 kPa) than that of the control (Group 1B; 1.85 ± 0.87 kPa) at day 21 post PTK ($p = 0.01$) (Figure 7). By contrast,

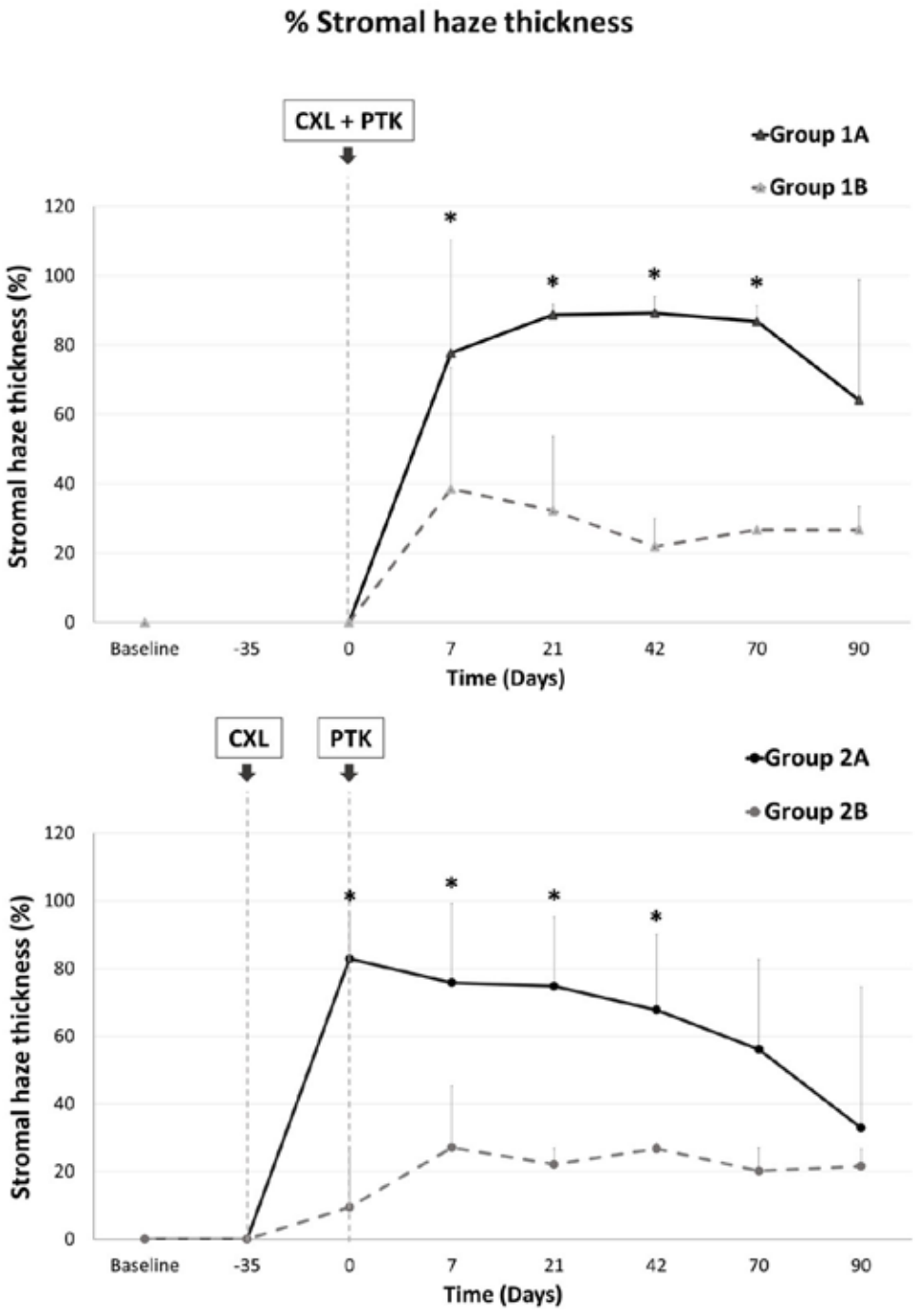

Figure 5. Stromal haze thickness as a function of time. Stromal haze thickness (%) of the central cornea was significantly higher in the CXL groups (1A and 2A) than in the controls (1B and 2B). No significant differences were observed between Group 1A and Group 2A. * $p < 0.05$, repeated measure two-way ANOVA followed by Tukey's multiple comparisons test.

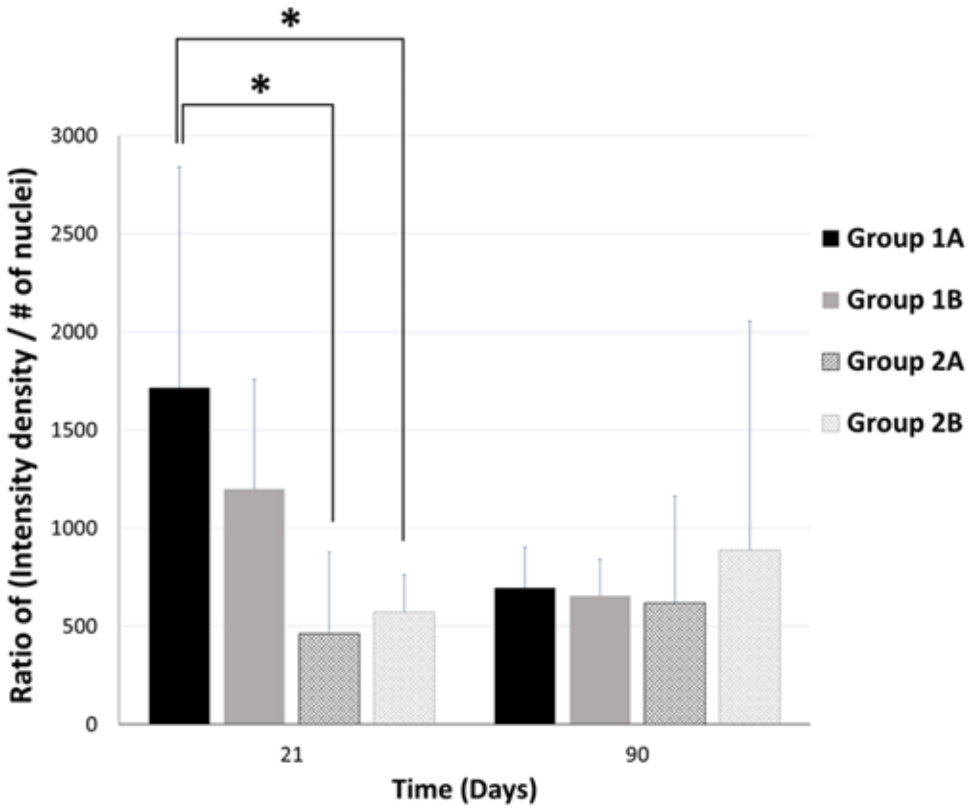

Figure 6. Intensity (intensity/mm^2) of the α-SMA immunofluorescence over the number of nuclei ± standard deviation in all groups at both day 21 and day 90 time points. Group 1A corneas had a significantly higher α-SMA immunofluorescence than had Groups 2A and 2B corneas at day 21, but they were similar by day 90. No significant differences were observed between any other groups at either time point. * p <0.05, two-way ANOVA followed by Sidak's multiple comparisons test).

there was no statistical difference between the mechanical properties of the CXL corneas of Groups 1A and 1B at day 90 (3.14 ± 1.01 kPa and 2.66 ± 0.73 kPa, respectively; p = 0.92). Moreover, there were no significant differences between Groups 2A (3.66 ± 2.61 kPa at day 21 and 2.67 ± 0.59 kPa at day 90) and 2B (1.93 ± 0.52 at day 21 and 2.77 ± 0.65 kPa at day 90) at both time points (p = 0.15 for day 21 and p = 0.95 for day 90).

DISCUSSION

By evaluating the elastic modulus of the corneal stroma, KFM transformation, and stromal haze formation following combined keratorefractive surgery and CXL in rabbits, we have provided evidence supportive of both our hypotheses, namely that CXL before PTK as well as simultaneous CXL–PTK increases stromal haze formation and that simultaneous CXL–PTK increases local corneal stiffness (day 21). Strikingly, stromal haze was similar between corneas receiving CXL concurrently with PTK versus those treated with CXL before PTK and markedly greater than those corneas treated by PTK only. Additionally, central corneal thickness significantly increased following CXL when performed concurrently with PTK and when performed before PTK. Finally, no significant differences were noted in time to epithelialization between groups following the procedures.

The introduction of CXL performed in combination with keratorefractive surgeries (most commonly laser-assisted in situ keratomileusis, or LASIK) has been widely reported to offer equivalent safety margins [10,31-33], improved refractive predictability [33-36], improved distance visual acuity [33,35,36], decreased regression of refractive shift [35,36], better refractive stability up to 4.5 years post-operatively [32,37], and decreased epithelial thickening [10,35]. Infrequent post-operative complications revolving around epithelial debridement, including pain [11], keratitis [12-16], persistent epithelial defects [17], and keratomalacia, have not curbed the use of CXL from becoming commonplace alongside keratorefractive surgery [9,18-20]. In the present study, pain was evident post-operatively and only persisted until the ulcer was deemed healed by a negative fluorescein stain. Additionally, no rabbits developed persistent epithelial defects, all having healed within 7 days post-operatively, and no cornea became infected or developed keratomalacia. Histologic evidence of keratitis was significantly more common in CXL corneas, compared with non-CXL corneas, at Day 21 but was absent by Day 90 in all cases.

Corneal opacity is frequently described post CXL and keratorefractive surgery, primarily due to early and transient corneal edema [21,22]. The development of corneal edema is most likely due to the epithelial defect, disrupting the fluid barrier normally provided by the anterior epithelium. Thus, corneal edema resolves with the resolution of the epithelial defect and without further delay. However, transient endothelial disruption cannot be ruled out, as endothelial damage following CXL has been shown to occur with 3 mW/cm^2 on corneas less than 400 um in thickness [38], which is consistent with our results. An increase in CCT due to edema was significantly increased in cross-linked corneas (Groups 1A and 2A), compared with those that were not crosslinked (Groups 1B and 2B), possibly indicating endothelial toxicity. PTK reduced the thickness of the cornea (100 um), and thus increases the likelihood of CXL impacting the endothelium. By contrast, Groups 1B and 2B did not have increased corneal thickness, which is suggestive that CXL itself is likely the cause of the transient corneal swelling due to endothelial disruption [38].

Stromal haze identified in human patients is also regularly noted in rabbits following CXL procedures and following combined CXL and keratorefractive surgery, typically with no effect on distance visual acuity [21,22,39]. However, the clinical characteristics and depth of the stromal haze following CXL have been described as different to those of stromal haze following keratorefractive surgery alone [21], and persistent haze or scars that negatively affect vision can occur [9,21,40]. In the present report, significant haze was evident on OCT for a greater duration than was evident by slit lamp biomicroscopic examination. OCT for routine monitoring of haze development and regression is recommended, considering the higher resolution for detecting haze at the microscopic level.

Risk factors for increased severity and persistence of stromal haze include keratoconus and thin corneas [41], stromal microstriae pre-operatively [22], and the presence of activated keratocytes in the anterior stroma before surgery [9,40]. No previously described risk factors were detected in any rabbit in the present study. The increase in stromal haze associated with the CXL groups, compared with the non-CXL groups, appears to be related to the CXL procedure itself in combination with simultaneous stromal wounding. A positive correlation between corneal mechanical strength and corneal stiffness is well documented as a direct result of the biomechanics of corneal wound repair [2,26,42-50]. This was confirmed in the present study through AFM, whereby the corneas in Group 1A were significantly stiffer than they were in Group 1B, supporting our first hypothesis. More specifically, the precise orchestration of keratocyte to fibroblast to myofibroblast differentiation (KFM transformation) and myofibroblast migration from bone marrow occurs as a direct result of an altered microenvironment due to stromal remodeling and biophysical cues [23-26,51-61]. Although

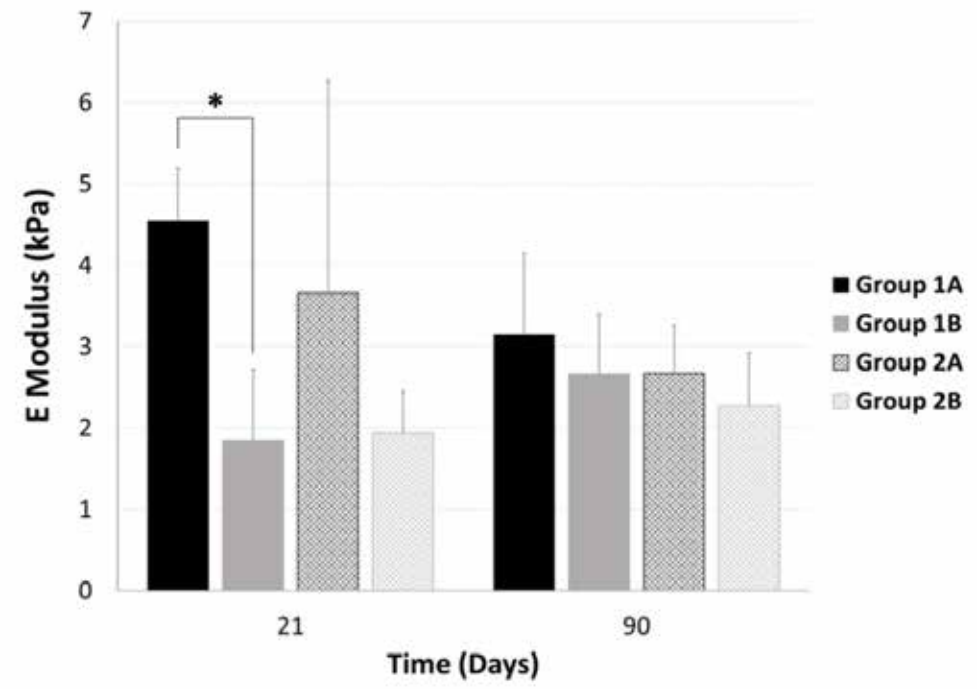

Figure 7. The elastic modulus of corneas having received CXL and PTK on the same day (Group 1A), PTK 35 days before CXL (Group 2A), and PTK only (Groups 1B and 2B). Group 1A corneas had a significantly higher elastic modulus than Group 1B corneas at day 21, but the elastic modulus was similar by day 90. However, no significant differences were observed between Group 2A and Group 2B at either time point. * p <0.05, two-way ANOVA followed by Tukey's multiple comparisons test).

the desired outcome of CXL is increased corneal stiffness, prolongation or dysregulation of the corneal wound healing process that results in increased myofibroblast transformation and stiffness can result in decreased corneal transparency (e.g., corneal scar or haze formation), and thus have a negative impact on visual acuity [26,62,63].

In the present study, a significantly greater amount of clinical stromal haze was noted in Groups 1A and 2A, compared with Groups 1B and 2B, from day 7 to day 70 and from day 7 to day 42, respectively, based on OCT data. This suggests that CXL impacts early post-operative haze formation, supporting our first hypothesis. Additionally, the amount of stromal haze was significantly greater in Group 2A, compared with Group 2B, until day 42, supporting our second hypothesis. The lack of significant difference in stromal haze between Groups 2A and 2B post day 42 fits the timeline exemplified in Group 1 (lack of significance past day 70), as Groups 2A and 2B had CXL performed 30 days before PTK, rather than CXL and PTK being performed simultaneously.

Identification of stromal haze by FD-OCT is a more sensitive measurement than clinical scoring and can be quantified (e.g., by the percentage of stromal thickness affected by haze). Stromal haze and densitometry have been shown to be highest at about 1 month post-operatively in rabbits [39] and humans [21,22], which is consistent with our findings across the CXL groups (days 21 and 42). Haze was visibly present in all groups to the end of the study, which is consistent with previous reports stating that stromal haze continually improves from 1 month to 12 months post-operatively, where it approaches baseline [21,22]. However, the severity of stromal haze noted in the present study is much greater than what has been reported in rabbits [38,39] or humans following CXL procedures [21,22]. This may be due to the higher number of natural crosslinks between stromal collagen fibers that rabbits have, compared with those of humans [2,43,44]. Rabbits have a higher proportion of collagen type 3, which has been shown to increase significantly following corneal crosslinking (compared with collagen type I), and thus rabbits may be predisposed to the development of greater stromal haze [64]. Additionally, the aforementioned studies did not assess corneas undergoing simultaneous CXL and keratorefractive surgeries, and thus stromal injury is likely responsible for the increased stromal haze formation.

Although the depth of stromal haze formation varied and approached full thickness in many individuals by day 21 following CXL, the amount of haze visualized by FD-OCT was more severe anteriorly, also likely due to simultaneous CXL and stromal injury (i.e., PTK). This is supported by previous studies, in which an increase in collagen fibril diameter compared to baseline was nearly threefold greater in the anterior stroma versus the posterior stroma [65]. The anterior stroma has also been recognized to develop keratocyte apoptosis up to a 300 um depth following epithelium-off CXL [38,65-67], especially compared with transepithelial CXL [68].

Additionally, a likely reason why a greater proportion of the rabbit cornea is affected by stromal haze formation compared with humans is due to rabbits' corneas being thinner. Previous studies have shown that riboflavin concentrations decrease with stromal depth [41,69-72], as does UVA light penetration [73]. Considering this, it has been suggested that CXL is only significantly impactful in the anterior stroma, where riboflavin and UVA concentrations are the highest [7,73]. However, the effects of CXL have been shown to reach the posterior stroma, as evidenced by increased collagen fibril diameter [64]. The depth of the stromal haze in the present study was much greater than previously published, nearly approaching full thickness in most cases. Increased depth of riboflavin penetration may be due to rabbit corneas being thinner than human corneas or due to rabbit corneas having a higher baseline crosslinking degree than human corneas [2,43,44].

In summary, by evaluating the elastic modulus of the corneal stroma and KFM transformation, we have shown that stromal haze formation and stromal stiffness following simultaneous keratorefractive surgery and CXL is marked in rabbits. We have also provided evidence that corneal stiffening by CXL leads to increased corneal scarring regardless of whether it is done at or before the time of PTK. Overall, further knowledge of the biophysical cues involved in determining corneal wound healing duration and outcomes will be important for understanding scarring following CXL and for the development of improved therapeutic options, and it should thus be incorporated into future studies [26,74,75].

ACKNOWLEDGMENTS

This work was supported by National Institutes of Health, National Eye Institute (US) Grants R01EY016134 (CJM), R01EY019970 (CJM), and P30EY12576 and by an unrestricted grant from Research to Prevent Blindness. VKR was supported partially by start-up funds at UHCO.

REFERENCES

1. Wollensak G, Spoerl E, Seiler T. Riboflavin/Ultraviolet-A-induced collagen crosslinking for the treatment of keratoconus. Am J Ophthalmol 2003; a135:620-7. [PMID: 12719068].
2. Wollensak G, Spoerl E, Seiler T. Stress-strain measurements of human and porcine corneas after riboflavin-ultraviolet-A-induced cross-linking. J Cataract Refract Surg 2003; b29:1780-5. [PMID: 14522301].
3. Wollensak G. Crosslinking treatment of progressive keratoconus: new hope. Curr Opin Ophthalmol 2006; 17:356-60. [PMID: 16900027].
4. McCall AS, Kraft S, Edelhauser HF, Kidder GW, Lundquist RR, Bradshaw HE, Dedeic Z, Dionne MJC, Clement EM, Conrad GW. Mechanisms of Corneal Tissue Cross-Linking in Response to Treatment with Topical Riboflavin and Long Wavelength Ultraviolet Radiation (UVA). Invest Ophthalmol Vis Sci 2010; 51:129-38. [PMID: 19643975].
5. Brummer G, Littlechild S, McCall S, Zhang Y, Conrad GW. The Role of Nonenzymatic Glycation and Carbonyls in Collagen Cross-Linking for the Treatment of Keratoconus. Invest Ophthalmol Vis Sci 2011; 52:6363-9. [PMID: 21724915].
6. Hayes S, Kamma-Lorger CS, Boote C, Young RD, Quantock AJ, Rost A, Khatib Y, Harris J, Yagi N, Terrill N, Meek KM. The effect of riboflavin/UVA collagen cross-linking therapy on the structure and hydrodynamic behaviour of the ungulate and rabbit corneal stroma. PLoS One 2013; 8:e52860[PMID: 23349690].
7. Dias J, Diakonis VF, Kankariya VP, Yoo SH, Ziebarth NM. Anterior and posterior corneal stroma elasticity after corneal collagen crosslinking treatment. Exp Eye Res 2013; 116:58-62. [PMID: 23933527].
8. Spoerl E, Huhle M, Seiler T. Induction of cross-links in corneal tissue. Exp Eye Res 1998; 66:97-103. [PMID: 9533835].
9. Evangelista CB, Hatch KM. Corneal collagen cross-linking complications. Semin Ophthalmol 2018; 33:29-35. [PMID: 28876968].
10. Tomita M. Combined laser in-situ keratomileusis and accelerated corneal cross-linking: an update. Curr Opin Ophthalmol 2016; 27:304-10. [PMID: 27152484].
11. Ghanem VC, Ghanem RC, De Oliveira R. Postoperative pain after corneal collagen cross-linking. Cornea 2013; 32:20-4. [PMID: 22547128].
12. Kymionis GD, Portaliou DM, Bouzoukis DI, Suh LH, Pallikaris AI, Markomanolakis M, Yoo SH. Herpetic keratitis with iritis after corneal crosslinking with riboflavin and ultraviolet A for keratoconus. J Cataract Refract Surg 2007; 33:1982-4. [PMID: 17964410].
13. Zamora KV, Males JJ. Polymicrobial keratitis after a collagen cross-linking procedure with postoperative use of a contact lens: A case report. Cornea 2009; 28:474-6. [PMID: 19411973].
14. Sharma N, Maharana P, Singh G, Titiyal JS. Pseudomonas keratitis after collagen crosslinking for keratoconus: Case report and review of literature. J Cataract Refract Surg 2010; 36:517-20. [PMID: 20202556].
15. Yuksel N, Bilgihan K, Hondur AM. Herpetic keratitis after corneal collagen cross-linking with riboflavin and ultraviolet-A for progressive keratoconus. Int Ophthalmol 2011; 31:513-5. [PMID: 22139351].
16. Abbouda A, Abicca I, Alió JL. Infectious keratitis following corneal crosslinking: A systematic review of reported cases: Management, visual outcome, and treatment proposed. Semin Ophthalmol 2016; 31:485-91. [PMID: 25392046].
17. Soeters N, Wisse RP, Godefrooij DA, Imhof SM, Tahzib NG. Transepithelial versus epithelium-off corneal cross-linking for the treatment of progressive keratoconus: A randomized controlled trial. Am J Ophthalmol 2015; 159:821-8.e3. [PMID: 25703475].
18. Labiris G, Kaloghianni E, Koukoula S, Zissimopoulos A, Kozobolis VP. Corneal melting after collagen cross-linking for keratoconus: A case report. J Med Case Rep 2011; 5:152-[PMID: 21496288].
19. Mohamed-Noriega K, Butrón-Valdez K, Vazquez-Galvan J, Mohamed-Noriega J, Cavazos-Adame H, Mohamed-Hamsho J. Corneal melting after collagen cross-linking for keratoconus in a thin cornea of a diabetic patient treated with topical nepafenac: A case report with a literature review. Case Rep Ophthalmol 2016; 7:119-24. [PMID: 27293413].
20. Chan TCY, Ng ALK, Chan KKW, Cheng GPM, Wong IYH, Jhanji V. Combined application of prophylactic corneal cross-linkings in-situ keratomileusis – a review of literature. Acta Ophthalmologica 2017; 95:660-4. [PMID: 27910295].
21. Koller T, Mrochen M, Seiler T. Complication and failure rates after corneal crosslinking. J Cataract Refract Surg 2009; 35:1358-62. [PMID: 19631120].
22. Mazzotta C, Balestrazzi A, Baiocchi S, Traversi C, Caporossi A. Stromal haze after combined riboflavin-UVA corneal collagen cross-linking in keratoconus: In vivo confocal microscopic evaluation. Clin Experiment Ophthalmol 2007; 35:580-2. [PMID: 17760642].
23. Pot SA, Liliensiek SJ, Myrna KE, Bentley E, Jester JV, Nealey PF, Murphy CJ. Nanoscale topography-induced modulation of fundamental cell behaviors of rabbit corneal keratocytes, fibroblasts, and myofibroblasts. Invest Ophthalmol Vis Sci 2010; 51:1373-81. [PMID: 19875665].
24. Myrna KE, Mendonsa R, Russell P, Pot SA, Liliensiek SJ, Jester JV, Nealey PF, Brown D, Murphey CJ. Substratum topography modulates corneal fibroblast to myofibroblast transformation. Invest Ophthalmol Vis Sci 2012; 53:811-6. [PMID: 22232431].
25. Dreier B, Thomasy SM, Mendonsa R, Raghunathan VK, Russell P, Murphy CJ. Substratum compliance modulates corneal fibroblast to myofibroblast transformation. Invest Ophthalmol Vis Sci 2013; 54:5901-7. [PMID: 23860754].

26. Raghunathan VK, Thomasy SM, Strom P, Yanez-Soto B, Garland SP, Sermeno J, Reilly CM, Murphy CJ. Tissue and cellular biomechanics during corneal wound injury and repair. Acta Biomater 2017; 58:291-301. [PMID: 28559158].

27. Eaton JS, Miller PE, Bentley E, Thomasy SM, Murphy CJ. The SPOTS System: An Ocular Scoring System Optimized for Use in Modern Preclinical Drug Development and Toxicology. J Ocul Pharmacol Ther 2017; 33:718-34. [PMID: 29239680].

28. Fantes FE, Hanna KD, Waring GO III, Pouliquen Y, Thompson KP, Savoldelli M. Wound healing after excimer laser keratomileusis (photorefractive keratectomy) in monkeys. Arch Ophthalmol 1990; 108:665-75. [PMID: 2334323].

29. Thomasy SM, Raghunathan VK, Winkler M, Reilly CM, Sadeli AR, Russell P, Jester JV, Murphy CJ. Elastic modulus and collagen organization of the rabbit cornea: epithelium to endothelium. Acta Biomater 2014; 10:785-91. [PMID: 24084333].

30. Hermann LR. Elasticity equations for incompressible and nearly incompressible materials by a variational theorem. Am Instit Aero Astro 1965; 3:1896-900. .

31. Celik HU, Alagoz N, Yildirim Y, Agca A, Marshall J, Demirok A, Yilmaz OF. Accelerated corneal crosslinking concurrent with laser in situ keratomileusis. J Cataract Refract Surg 2012; 38:1424-31. [PMID: 22814049].

32. Kanellopoulos AJ, Kahn J. Topography-guided hyperopic LASIK with and without high irradiance collagen crosslinking: initial comparative clinical findings in a contralateral eye study of 34 consecutive patients. J Refract Surg 2012; 28:S837-40. [PMID: 23447898].

33. Tomita M, Yoshida Y, Yamamoto Y, Mita M, Waring IVG. In vivo confocal laser microscopy of morphologic changes after simultaneous LASIK and accelerated collagen crosslinking for myopia: one-year results. J Cataract Refract Surg 2014; 40:981-90. [PMID: 24857441].

34. Tan J, Lytle GE, Marshall J. Consecutive laser in situ keratomileusis and accelerated corneal crosslinking in highly myopic patients: preliminary results. Eur J Ophthalmol 2014; 25:101-7. [PMID: 25588591].

35. Kanellopoulos AJ, Asimellis G, Karabatsas C. Comparison of prophylactic higher fluence corneal cross-linking to control, in myopic LASIK, one year results. Clin Ophthalmol 2014; 8:2373-81. [PMID: 25473264].

36. Kanellopoulos AJ, Asimellis G. Combined laser in situ keratomileusis and prophylactic high-fluence corneal collagen crosslinking for high myopia: two-year safety and efficacy. J Cataract Refract Surg 2015; 41:1426-33. [PMID: 26287881].

37. Aslanides IM, Mukherjee AN. Adjuvant corneal crosslinking to prevent hyperopic LASIK regression. Clin Ophthalmol 2013; 7:637-41. [PMID: 23576861].

38. Zhu Y, Reinach PS, Zhu H, Li L, Yang F, Qu J, Chen W. Continuous-light versus pulsed-light accelerated corneal crosslinking with ultraviolet-A and riboflavin. J Cataract Refract Surg 2018; 44:382-9. [PMID: 29703291].

39. Bradford SM, Mikula ER, Juhasz T, Brown DJ, Jester JV. Collagen fiber crimping following in vivo UVA-induced corneal crosslinking. Exp Eye Res 2018; 177:173-80. [PMID: 30118656].

40. Mazzotta C, Hafezi F, Kymionis G, Caragiuli S, Jacob S, Traversi C, Barabino S, Randleman JB. In vivo confocal microscopy after corneal collagen crosslinking. Ocul Surf 2015; 13:298-314. [PMID: 26142059].

41. Raiskup F, Hoyer A, Spoerl E. Permanent corneal haze after riboflavin-UVA-induced cross-linking in keratoconus. J Refract Surg 2009; 25:S824-8. [PMID: 19772259].

42. Tomkins O, Garzozi HJ. Collagen cross-linking: strengthening the unstable cornea. Clin Ophthalmol 2008; 2:863-7. [PMID: 19668440].

43. Wollensak G, Iomdina E. Biomechanical and histological changes after corneal crosslinking with and without epithelial debridement. J Cataract Refract Surg 2009; a35:540-6. [PMID: 19251149].

44. Wollensak G, Iomdina E. Long-term biomechanical properties of rabbit cornea after photodynamic collagen crosslinking. Acta Ophthalmol 2009; b87:48-51. [PMID: 18547280].

45. Kling S, Remon L, Perez-Escudero A, Merayo-Lloves J, Marcos S. Corneal biomechanical changes after collagen cross-linking from porcine eye inflation experiments. Invest Ophthalmol Vis Sci 2010; 51:3961-8. [PMID: 20335615].

46. Schumacher S, Oeftiger L, Mrochen M. Equivalence of biomechanical changes induced by rapid and standard corneal cross-linking, using riboflavin and ultraviolet radiation. Invest Ophthalmol Vis Sci 2011; 52:9048-52. [PMID: 22025568].

47. Lanchares E, del Buey MA, Cristobal JA, Lavilla L, Calvo B. Biomechanical property analysis after corneal collagen cross-linking in relation to ultraviolet A irradiation time. Graefes Arch Clin Exp Ophthalmol 2011; 249:1223-7. [PMID: 21494876].

48. Cherfan D, Verter EE, Melki S, Gisel TE, Doyle FJ Jr, Scarcelli G, Yun SH, Redmond RW, Kochevar IE. Collagen cross-linking using rose bengal and green light to increase corneal stiffness. Invest Ophthalmol Vis Sci 2013; 54:3426-33. [PMID: 23599326].

49. Scarcelli G, Kling S, Quijano E, Pineda R, Marcos S, Yun SH. Brillouin microscopy of collagen crosslinking: noncontact depth-dependent analysis of corneal elastic modulus. Invest Ophthalmol Vis Sci 2013; 54:1418-25. [PMID: 23361513].

50. Thomasy SM, Raghunathan VK, Miyagi H, Evashenk AT, Sermeno JC, Tripp GK, Morgan JT, Murphy CJ. Latrunculin B and substratum stiffness regulate corneal fibroblast to myofibroblast transformation. Exp Eye Res 2018; 170:101-7. [PMID: 29421383].

51. Myrna KE, Pot SA, Murphy CJ. Meet the corneal myofibroblast: the role of myofibroblast transformation in corneal

wound healing and pathology. Vet Ophthalmol 2009; 12:25-7. [PMID: 19891648].

52. Barbosa FL, Chaurasia SS, Cutler A, Asosingh K, Kaur H, de Medeiros FW, Agrawal V, Wilson SE. Corneal myofibroblast generation from bone marrow-derived cells. Exp Eye Res 2010; 91:92-6. [PMID: 20417632].

53. Fini ME. Keratocyte and fibroblast phenotypes in the repairing cornea. Prog Retin Eye Res 1999; 18:529-51. [PMID: 10217482].

54. Torricelli AA, Wilson SE. Cellular and extracellular matrix modulation of corneal stromal opacity. Exp Eye Res 2014; 129:151-60. [PMID: 25281830].

55. Fraser SA, Ting YH, Mallon KS, Wendt AE, Murphy CJ, Nealey PF. Sub-micron and nanoscale feature depth modulates alignment of stromal fibroblasts and corneal epithelial cells in serum-rich and serum-free media. J Biomed Mater Res A 2008; 86:725-35. [PMID: 18041718].

56. Tocce EJ, Smirnov VK, Kibalov DS, Liliensiek SJ, Murphy CJ, Nealey PF. The ability of corneal epithelial cells to recognize high aspect ratio nanostructures. Biomaterials 2010; 31:4064-72. [PMID: 20153044].

57. Karuri NW, Liliensiek S, Teixeira AI, Abrams G, Campbell S, Nealey PF, Murphy CJ. Biological length scale topography enhances cell-substratum adhesion of human corneal epithelial cells. J Cell Sci 2004; 117:3153-64. [PMID: 15226393].

58. Karuri NW, Porri TJ, Albrecht RM, Murphy CJ, Nealey PF. Nano- and microscale holes modulate cell-substrate adhesion, cytoskeletal organization, and beta1 integrin localization in SV40 human corneal epithelial cells. IEEE Trans Nanobioscience 2006; 5:273-80. [PMID: 17181027].

59. Liliensiek SJ, Campbell S, Nealey PF, Murphy CJ. The scale of substratum topographic features modulates proliferation of corneal epithelial cells and corneal fibroblasts. J Biomed Mater Res A 2006; 79:185-92. [PMID: 16817223].

60. Yanez-Soto B, Liliensiek SJ, Gasiorowski JZ, Murphy CJ, Nealey PF. The influence of substrate topography on the migration of corneal epithelial wound borders. Biomaterials 2013; b34:9244-51. [PMID: 24016856].

61. Yanez-Soto B, Liliensiek SJ, Murphy CJ, Nealey PF. Biochemically and topographically engineered poly(ethylene glycol) diacrylate hydrogels with biomimetic characteristics as substrates for human corneal epithelial cells. J Biomed Mater Res A 2013; a101:1184-94. [PMID: 23255502].

62. Jester JV, Budge A, Fisher S, Huang J. Corneal keratocytes: phenotypic and species differences in abundant protein expression and in vitro light-scattering. Invest Ophthalmol Vis Sci 2005; 46:2369-78. [PMID: 15980224].

63. Jester JV, Huang J, Barry-Lane PA, Kao WW, Petroll WM, Cavanagh HD. Transforming growth factor$_b$–mediated corneal myofibroblast differentiation requires actin and fibronectin assembly. Invest Ophthalmol Vis Sci 1999; 40:1959-67. [PMID: 10440249].

64. Xia Y, Liu B, Fan Z, Peng X. Corneal collagen fibril changes after ultraviolet A/Riboflavin corneal crosslinking. Cornea 2014; 33:56-9. [PMID: 24240489].

65. Wollensak G, Spoerl E, Wilsch M, Seiler T. Keratocyte apoptosis after corneal collagen cross-linking using Riboflavin/UVA treatment. Cornea 2004; 23:43-9. [PMID: 14701957].

66. Podskochy A, Gan L, Fagerholm P. Apoptosis in UV-exposed rabbit corneas. Cornea 2000; 19:99-103. [PMID: 10632017].

67. Ozmen MC, Hondur A, Yilmaz G, Bilgihan K, Hasanreisoglu B. A histological study of rabbit corneas after transepithelial corneal crosslinking using partial epithelial photoablation or ethanol treatment. Int J Ophthalmol 2014; 7:959-63. [PMID: 25540746].

68. Armstrong BK, Lin MP, Ford MR, Santhiago MR, Singh V, Grossman GH, Agrawal V, Sinha RA, Butler RS, Dupps WJ, Wilson SE. Biological and biomechanical responses to traditional epithelium-off and transepithelial riboflavin-UVA CXL techniques in rabbits. J Refract Surg 2013; 29:332-41. [PMID: 23659231].

69. Wollensak G, Aurich H, Wirbelauer C, Sel S. Significance of the riboflavin film in corneal collagen crosslinking. J Cataract Refract Surg 2010; 36:114-20. [PMID: 20117714].

70. Sondergaard AP, Hjortdal J, Breitenbach T, Ivarsen A. Corneal Distribution of Riboflavin prior to Collagen Cross-Linking. Curr Eye Res 2010; 35:116-21. [PMID: 20136421].

71. Spoerl E, Mrochen M, Sliney D, Trokel S, Seiler T. Safety of UVA-Riboflavin Cross-Linking of the Cornea. Cornea 2007; 26:385-9. [PMID: 17457183].

72. Spoerl E, Raiskup F, Kampik D, Geerling G. Correlation between UV Absorption and Riboflavin Concentration in Different Depths of the Cornea in CXL. Curr Eye Res 2010; 35:1040-1. [PMID: 20958193].

73. Kohlhaas M, Spoerl E, Schilde T, Unger G, Wittig C, Pillunat LE. Biomechanical evidence of the distribution of cross-links in corneas treated with riboflavin and ultraviolet A light. J Cataract Refract Surg 2006; 32:279-83. [PMID: 16565005].

74. Esquenazi S, He J, Li N, Bazan HEP. Immunofluorescence of rabbit corneas after collagen cross-linking treatment with riboflavin and ultraviolet A. Cornea 2010; 29:412-7. [PMID: 20164740].

75. Mastropasqua L, Nubile M, Calienno R, Mattei PA, Pedrotti E, Salgari N, Mastropasqua R, Lanzini M. Corneal cross-linking: intrastromal riboflavin concentration in iontophoresis-assisted imbibition versus traditional and transepithelial techniques. Am J Ophthalmol 2014; 157:623-30.e1. [PMID: 24321474].

Articles are provided courtesy of Emory University and the Zhongshan Ophthalmic Center, Sun Yat-sen University, P.R. China. The print version of this article was created on 16 July 2023. This reflects all typographical corrections and errata to the article through that date. Details of any changes may be found in the online version of the article.